International Journal for Vitamin and Nutrition Research

Int. J. Vitam. Nutr. Res. **2025**; 95(4): 37311
https://doi.org/10.31083/IJVNR37311

Original Communication

Low-protein Calorie-restriction Mitigates Diabetic Mice Kidney Injury via the Gut–Kidney Axis

Ruixiang Zhang[1,2,†], Xiao Wei[1,†], Yijiao Xu[1], Chunrong Han[3], Xiangzeng Cai[4], Yinling Wu[4], Yan Geng[4,*], Chao Liu[1,*]

[1]Department of Endocrinology, Affiliated Hospital of Integrated Chinese and Western Medicine, Nanjing University of Chinese Medicine, 210028 Nanjing, Jiangsu, China
[2]Division of Endocrinology, Department of Internal Medicine, Tongji Hospital, Tongji Medical College, Huazhong University of Science and Technology, 430030 Wuhan, Hubei, China
[3]Department of Pathology, Nanjing Lishui People's Hospital, Zhongda Hospital Lishui Branch, Southeast University, 211200 Nanjing, Jiangsu, China
[4]Department of Endocrinology, Nanjing Lishui People's Hospital, Zhongda Hospital Lishui Branch, Southeast University, 211200 Nanjing, Jiangsu, China
*Correspondence: gengyan2004@163.com (Yan Geng); profliuchao@163.com (Chao Liu)
[†]These authors contributed equally.
Academic Editor: Torsten Bohn
Submitted: 21 January 2025 Revised: 22 April 2025 Accepted: 13 May 2025 Published: 27 August 2025

Abstract

Background: Dietary interventions have exhibited promise in restoring microbial balance in chronic kidney disease. A low-protein calorie-restricted diet can reduce kidney injury in diabetic rodents. However, whether the renoprotective effects of this dietary intervention in murine diabetic kidney disease models are linked to gut microbiota modulation remains to be determined. **Methods**: Diabetic mice (induced by high-fat diet and streptozotocin) were randomized into four groups (n = 8/group): normal protein (20% protein), caloric restriction (30% restriction), low-protein (13% protein), and low-protein calorie-restricted (13% protein + 30% restriction). After a 5-week intervention, blood and urine samples were collected for relevant analyses, fecal samples for gut microbiota analysis, and kidney tissues for histological, immunohistochemical, and Western immunoblotting assays. **Results**: The low-protein calorie-restricted diet significantly improved glycemic control (fasting blood glucose: $p < 0.01$), ameliorated dyslipidemia (all $p < 0.01$), and mitigated kidney damage in diabetic mice. Additionally, the low-protein calorie-restricted diet ameliorated gut microbiota dysbiosis, significantly suppressing the increase in Firmicutes/Bacteroidetes ratio ($p = 0.02$) and decreasing serum trimethylamine oxide levels (67.51 $\pm$ 1.47 ng/mL vs. 56.58 $\pm$ 5.75 ng/mL; $p < 0.01$). Compared to the normal protein group, the low-protein calorie-restricted group exhibited significant reductions in serum tumor necrosis factor-α (TNF-α) levels (20.75 $\pm$ 7.83 µmol/L vs. 5.37 $\pm$ 2.45 µmol/L; $p < 0.01$) and apoptosis-associated speck-like protein containing a CARD (ASC), NOD-like receptor family pyrin domain containing 3 (NLRP3), and interleukin-1β (IL-1β) expression in kidney tissue (all $p < 0.01$). **Conclusions**: The low-protein calorie-restricted diet exerts renoprotective effects in mice with diabetic kidney disease, possibly by modulating the gut–kidney axis to reduce circulating trimethylamine oxide levels, suggesting a potential link to NLRP3 inflammasome suppression in kidney tissue.

Keywords: low-protein diet; caloric restriction; gut microbiota; diabetic kidney disease

1. Introduction

Diabetic kidney disease (DKD), a prevalent chronic complication of diabetes, remains a leading contributor to end-stage renal disease and cardiovascular mortality globally [1]. DKD has a complex pathogenesis, and its clinical treatment options are limited. In addition to haemodynamic abnormalities, overactivation of the renin–angiotensin system, inflammation, podocyte injury, and autophagy, gut microbiota and their metabolites contribute to the pathogenesis of DKD [1,2]. Emerging evidence highlights the gut microbiota's metabolic interplay with renal pathophysiology—termed the gut–kidney axis [3]—as a novel therapeutic frontier for DKD management.

A low-protein diet is the primary clinical approach for managing DKD, offering renal protection by reducing glomerular hyperfiltration and hypertension and improving tubular interstitial injury, inflammation, and fibrosis [4]. Caloric restriction (CR) is acknowledged for its anti-aging properties and metabolic benefits [5] and has demonstrated renoprotective effects [6]. For example, CR alleviates kidney damage in rodents with type 2 diabetes [7,8] and enhances kidney function in individuals with obesity with type 2 diabetes [9,10]. A low-protein, calorie-restricted (LPCR) diet mitigated renal damage in rodents with type 2 diabetes [11].

Gut microbiota is vital for human health, and its composition and function are affected by various factors, such as diet, disease, and antibiotic use [12]. CR can alter the gut microbiota composition with varying effects based on dietary components [13]. A low-protein diet lowers uraemic toxin levels in individuals with chronic kidney dis-

ease (CKD) by modulating the gut microbiota [14]. Despite existing evidence, the potential of LPCR diet to mitigate diabetic nephropathy through microbiota-driven mechanisms remains unexplored.

This study employed a high-fat diet/streptozotocin-induced diabetic murine model to evaluate the renoprotective efficacy of LPCR intervention, with specific emphasis on exploring the mediatory role of gut microbiota in this therapeutic process.

2. Materials and Methods

2.1 Animals

Specific pathogen-free male C57BL/6J mice (6–8 weeks old, 17–21 g) were obtained from SPF Biotechnology Co., Ltd. (Suzhou, China; Permit No. SYXK [SU] 2021-0025) and maintained under standardized conditions (24 $\pm$ 2 °C, 12-h light/dark cycle) with ad libitum water access. Notably, the mice underwent a one-week acclimatisation period prior to the commencement of the study. All procedures were conducted in accordance with the Guidelines for the Care and Use of Animals established by the Chinese Animal Management Committee, as approved by the Animal Experiment Ethics Committee of the Affiliated Hospital of Nanjing University of Chinese Medicine (Ethics No. AEWC-20230531-309).

2.2 Model Construction and Study Design

After a week of acclimatisation, mice were divided into two cohorts: the normal control (NC) group (n = 8, housed 4 per cage) received a standard diet, while the remaining 32 animals were subjected to a 12-week high-fat diet. Diabetes was subsequently induced via intraperitoneal administration of streptozotocin (S0130, Sigma-Aldrich, St. Louis, MO, USA; 40 mg/kg/day $\times$ 4 days). After the injections, the mice were continued on the high-fat diet. Mice with fasting blood glucose (FBG) levels $\geq$16.7 mmol/L at 10 weeks after streptozotocin injection were considered to have diabetes. Thereafter, diabetic mice were randomized into four groups (n = 8/group, housed 4 per cage): normal protein (NP, 20% protein), CR (30% restriction), low-protein (LP, 13% protein), and LPCR (13% protein + 30% restriction). All diets (Jiangsu Xietong Pharmaceutical Bioengineer Co., Ltd.) were formulated as detailed in **Supplementary Table 1**. Daily food intake was measured, and FBG and body weight were recorded weekly, with dietary intervention lasting for a total of five weeks (Fig. 1).

2.3 Sample Collection and Indicator Detection

After a five-week period of dietary intervention, random urine samples were obtained from the mice using individual metabolic cages, followed by the determination of urinary albumin (LA128107H, Nanjing Jin Yibai Biological Technology Co., Ltd, Nanjing, Jiangsu, China) and creatinine (C011-2-1, Nanjing Jiancheng Bioengineering Institute, Nanjing, Jiangsu, China) levels using enzyme-linked immunosorbent assay (ELISA). Retro-orbital blood samples were centrifuged (4 °C, 1000 g for 15 min) to extract serum. Serum creatinine, triglycerides (TG) (A110-1-1, Nanjing Jiancheng Bioengineering Institute, Nanjing, Jiangsu, China), total cholesterol (T-CHO) (A111-1-1, Nanjing Jiancheng Bioengineering Institute, Nanjing, Jiangsu, China), low-density lipoprotein cholesterol (LDL-C) (A113-1-1, Nanjing Jiancheng Bioengineering Institute, Nanjing, Jiangsu, China), high-density lipoprotein cholesterol (HDL-C) (A112-1-1, Nanjing Jiancheng Bioengineering Institute, Nanjing, Jiangsu, China), glutathione (GSH) (A006-2-1, Nanjing Jiancheng Bioengineering Institute, Nanjing, Jiangsu, China), superoxide dismutase (SOD) (A011-3-2, Nanjing Jiancheng Bioengineering Institute, Nanjing, Jiangsu, China), trimethylamine oxide (TMAO) (MM-1122M1, Elabscience Biotechnology Co., Ltd, Wuhan, Hubei, China), and tumor necrosis factor-α (TNF-α) (H052-1-2, Nanjing Jiancheng Bioengineering Institute, Nanjing, Jiangsu, China) levels were determined using ELISA kits.

At the end of the experiment, mice were anaesthetised with pentobarbital sodium (30 mg/mL, 100 mg/kg, i.p.) (CAS: 57-33-0, Department of Pharmacy, Affiliated Hospital of Integrated Chinese and Western Medicine, Nanjing University of Chinese Medicine). All mice were humanely euthanized at the conclusion of the experiment using the method of cervical dislocation. Intestinal feces were collected, rapidly frozen in liquid nitrogen, and transported in dry ice to Majorbio Bio-Pharm Technology Co., Ltd. for gut microbiota analysis. Kidney samples were divided into two portions, either fixed in 4% paraformaldehyde (G1101, Servicebio, Wuhan, Hubei, China) for histopathological examination or stored at –80 °C for western blotting.

2.4 Histopathology and Immunohistochemistry

Paraffin-embedded renal tissue sections (4 µm thickness) were prepared and subjected to staining with haematoxylin and eosin, periodic acid-Schiff, and Masson's trichrome for structural evaluation. For Masson's trichrome staining, the extent of collagen fiber deposition (blue-stained areas) was quantitatively analyzed using ImageJ software (National Institutes of Health, Bethesda, MD, USA). For immunohistochemical assay, the sections were probed with rabbit polyclonal antibodies targeting fibronectin (Cat No.15613-1-AP, proteintech, Wuhan, Hubei, China) (1:200) and collagen I (Cat No.14695-1-AP, proteintech, Wuhan, Hubei, China) (1:200) overnight at 4 °C, followed by incubation with horseradish peroxidase-conjugated goat anti-rabbit secondary antibody (Cat No. SA00001-2, proteintech, Wuhan, Hubei, China) at room temperature for 30 min. The expression levels of fibronectin and collagen I were analysed quantitatively using ImageJ software.

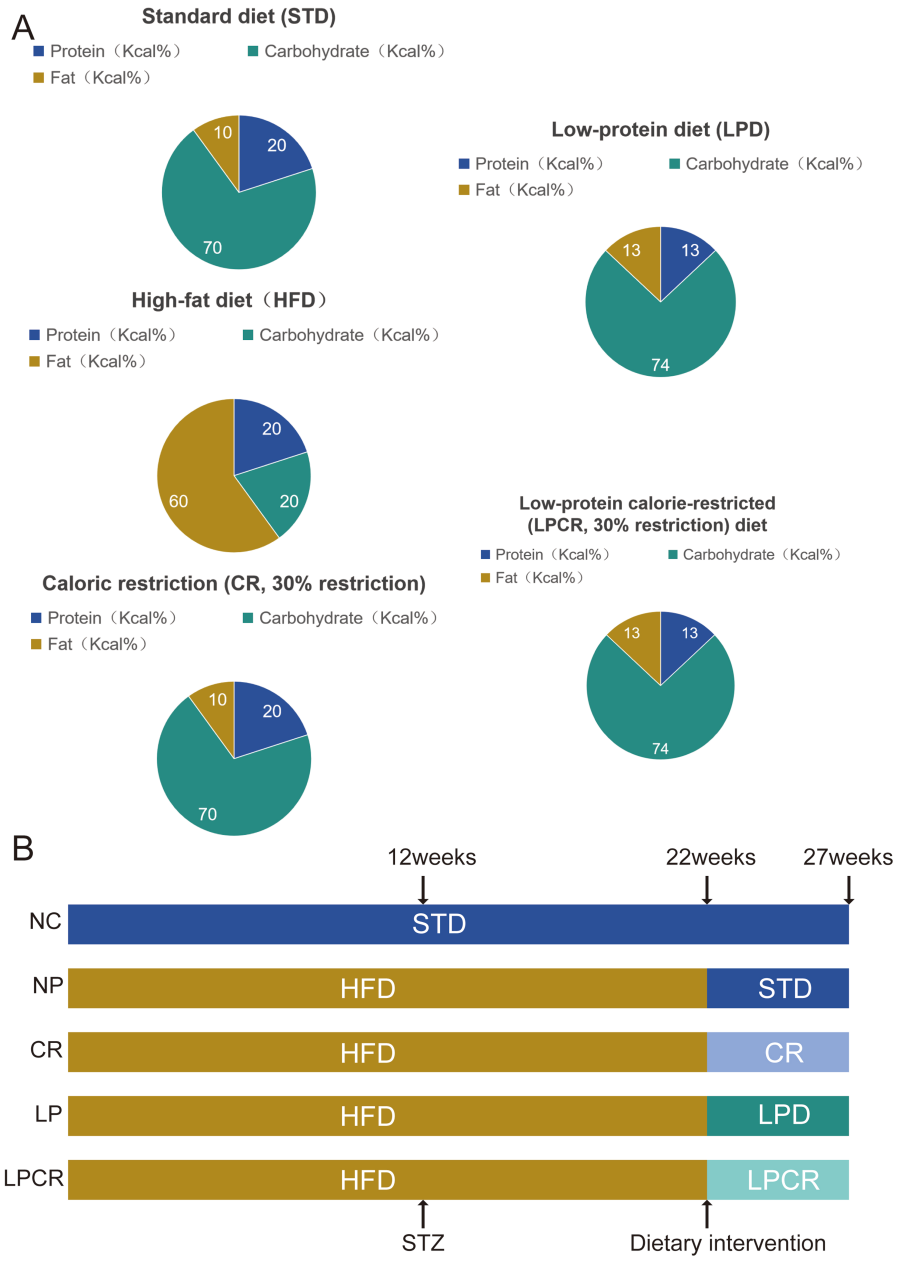

Fig. 1. Dietary paradigms and study design. (A) Dietary composition (green: carbohydrate, brown: fat, blue: protein). Standard diet (STD) provided 70% of calories from carbohydrates, 10% from fat, and 20% from protein. High-fat diet (HFD) provided 60% of calories from fat, 20% from carbohydrates, and 20% from protein. Caloric restriction (CR) consisted of a 30% reduction in total calories from the STD (i.e., 70% of STD calories). Low-protein diet (LPD) provided 13% of calories from protein, 74% from carbohydrates, and 13% from fat. Low-protein calorie-restricted (LPCR) diet combined the LPD with a 30% caloric restriction (i.e., 70% of LPD calories). (B) Study design. Eight mice assigned to normal control (NC) group were maintained on a STD. A mouse model of diabetes was established by feeding the mice a 12-week HFD, followed by multiple intraperitoneal injections of streptozotocin (STZ), and an additional 10 weeks of HFD. The diabetic mice were randomized into four groups: a normal protein (NP) group fed STD, and three groups receiving dietary interventions of CR, low-protein (LP), and LPCR (n = 8 mice/group). After 5 weeks of dietary intervention, blood, urine, fecal samples, and kidney tissues were collected for relevant analyses.

2.5 Gut Microbiome Analysis

Microbial genomic DNA was isolated from fecal samples using the PF Mag-Bind Stool DNA Kit (M5635-02, Omega Bio-tek, Norcross, GA, USA). DNA purity and concentration were assessed using a Nanodrop 2000 spectrophotometer (Thermo Scientific, Waltham, MA, USA). Qualified DNA samples were subjected to amplification of the *16S* rRNA gene. PCR was performed

with custom universal primers: forward primers 27F (5′-AGRGTTYGATYMTGGCTCAG-3′) and reverse primer 1492R (5′-RGYTACCTTGTTACGACTT-3′). The optimized thermal cycling protocol included initial denaturation at 95 °C for 180 s, followed by 27 cycles of denaturation (95 °C, 30 s), annealing at 60 °C (30 s), extension (72 °C, 45 s), and a final extension at 72 °C for 600 s. Subsequently, a PacBio library was constructed and sequenced. PacBio data were analysed using SMRTLink 11.0 (Pacific Biosciences, Menlo Park, CA, USA), resulting in at least three complete passes with 99% sequence accuracy for high-fidelity sequences. High-fidelity sequences were processed using UPARSE 11 (Drive5, Sonoma, CA, USA) to classify the operational taxonomic units at 97% similarity.

The Gut Microbiome Health Index (GMHI) was calculated to quantitatively assess the microbial community health potential, the formula was constructed based on the theoretical framework proposed by Gupta *et al.* [15]. Permutational multivariate analysis of variance (PERMANOVA; 999 permutations, Bray-Curtis distance) was performed to test the significance of differences in gut microbiota composition among the dietary intervention groups. Principal coordinate analysis (PCoA) was performed to derive key coordinates and display sample variations in a multidimensional space, and visualizations were generated using the R software (Version 3.3.1, R Development Core Team, Auckland, New Zealand).

2.6 Western Blotting

Proteins were extracted frozen kidney tissues, mixed with western blotting loading buffer, separated using SDS-PAGE (P0012A, Beyotime, Shanghai, China). After electrophoretic separation, samples were transferred onto PVDF membranes. The membranes were blocked with 5% skim milk for 2 h at room temperature, followed by overnight incubation at 4 °C with primary antibodies targeting apoptosis-associated speck-like protein containing a CARD (ASC) (Cat No.67824, CST, Boston, MA, USA), NOD-like receptor family pyrin domain containing 3 (NLRP3) (Cat No.15101, CST, Boston, MA, USA), interleukin-1β (IL-1β) (Cat No.31202, CST, Boston, MA, USA), and β-actin (Cat No.3700, CST, Boston, MA, USA) (all diluted at 1:3000). Subsequently, membranes were washed and incubated with species-matched horseradish peroxidase-conjugated secondary antibodies (anti-rabbit: Cat No.7074, CST, Boston, MA, USA; anti-mouse: Cat No.7076, CST, Boston, MA, USA) at 4 °C for 48 h. Protein bands were visualized using a chemiluminescent detection system, and quantitative densitometry was performed using the ImageJ software (National Institutes of Health, Bethesda, MD, USA).

2.7 Statistical Analysis

Data analysis was conducted using GraphPad Prism 8.0.2 (GraphPad Software, Inc., San Diego, CA, USA). Normally distributed variables are presented as mean $\pm$ SD. Normality was assessed using the Shapiro-Wilk test. For homogeneity of variances, either Bartlett's or Brown-Forsythe test was employed depending on the normality test outcome. For parametric comparisons across multiple groups, one-way ANOVA followed by Tukey's post-hoc test was applied. Nonparametric comparisons between the two groups were conducted using the Mann–Whitney U test, followed by false discovery rate correction for multiple comparisons. A p-value < 0.05 was considered statistically significant.

3. Results

3.1 LPCR Diet Improves Glucose and Lipid Metabolism

Table 1 summarises the changes in body weight and FBG levels across the different groups before and after the dietary intervention. At the experimental endpoint, diabetic mice across the intervention groups exhibited markedly reduced body weights relative to the NC group (all $p < 0.01$). Although the body weight in the LPCR group displayed a downward trend compared with the NP group, this difference was not statistically significant. All three dietary intervention groups experienced a reduction in FBG levels compared with that at baseline, whereas the NP group showed an increase. Notably, FBG levels were significantly lower in the LP and LPCR groups than in the NP group at the end of the intervention (both $p < 0.01$).

After five weeks of dietary intervention, the NP group exhibited marked elevations in serum TG, T-CHO, and LDL-C (all $p < 0.01$) alongside a reduction in HDL-C ($p = 0.023$) relative to the NC group. However, LP and LPCR diets significantly improved the levels of all four lipid parameters compared to the NP group (all $p < 0.01$), with the LPCR intervention displaying superior efficacy in modulating LDL-C and HDL-C profiles (Fig. 2).

3.2 LPCR Diet Mitigates Kidney Damage

To examine the effects of LPCR on kidney function, we measured serum creatinine concentrations and urinary albumin-to-creatinine ratios after five weeks of dietary intervention. The NP group exhibited significantly elevated serum creatinine levels and urinary albumin-to-creatinine ratios relative to the NC group (both $p < 0.01$). In contrast, the three dietary interventions showed substantial reductions in both serum creatinine levels and urinary albumin-to-creatinine ratios compared to NP group measurements (all $p < 0.01$; Fig. 3).

Haematoxylin and eosin staining revealed that mice in the NP group exhibited pathological changes characteristic of DKD, including irregular glomerular morphology, cytoplasmic vacuolation of renal tubular epithelial cells, and

Table 1. LPCR diet modulates body weights and fasting blood glucose levels in diabetic mice at 22 and 27 weeks.

Group	Body weight (g)		Weight change	Fasting blood glucose (mmol/L)		Glucose change
	22 w	27 w		22 w	27 w	
NC	26.18 ± 1.59	27.00 ± 1.85	0.82 ± 2.19	7.00 ± 0.76	7.05 ± 0.57	0.05 ± 1.01
NP	25.94 ± 2.80	22.04 ± 1.34**	–3.90 ± 2.74**	22.50 ± 6.21**	27.89 ± 3.70**	5.39 ± 4.93
CR	25.80 ± 1.70	21.14 ± 2.45**	–4.66 ± 2.36**	27.84 ± 3.34**	24.18 ± 5.17**	–3.66 ± 6.68$^{\#}$
LP	25.88 ± 2.25	21.35 ± 1.81**	–4.53 ± 2.88**	25.43 ± 4.43**	15.29 ± 6.03*$^{\#\#}$	–10.14 ± 5.98**$^{\#\#}$
LPCR	25.69 ± 1.15	19.80 ± 2.74**	–5.89 ± 2.90**	20.98 ± 6.25**	15.71 ± 6.45**$^{\#\#}$	–5.27 ± 7.33$^{\#\#}$

Pre- and post-intervention changes (22- and 27-week timepoints) in diabetic mice. Values are expressed as mean ± SD, $n = 8$. *$p < 0.05$, **$p < 0.01$ vs. NC group; $^{\#}p < 0.05$, $^{\#\#}p < 0.01$ vs. NP group. LPCR, low-protein calorie-restricted; NC, normal control; NP, normal protein; CR, caloric restriction; LP, low-protein.

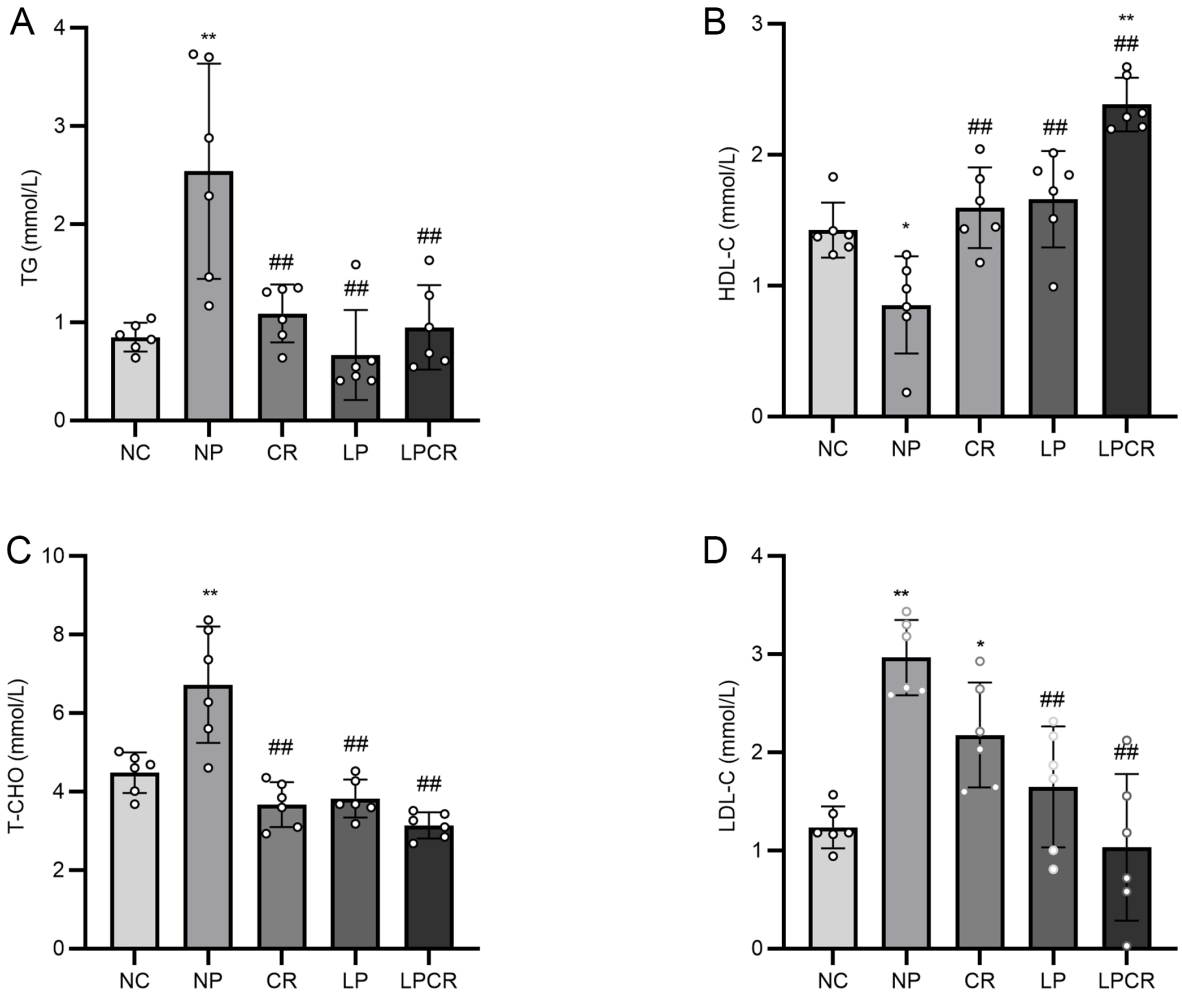

Fig. 2. LPCR diet improves lipid metabolism in DKD mice. (A) Mean TG level, (B) mean HDL-C level, (C) mean T-CHO level, and (D) mean LDL-C level in each group after dietary intervention. Values are expressed as mean ± SD, $n = 6$. *$p < 0.05$, **$p < 0.01$ vs. NC group; $^{\#\#}p < 0.01$ vs. NP group. LPCR, low-protein calorie-restricted; DKD, diabetic kidney disease; TG, triglycerides; HDL-C, high-density lipoprotein cholesterol; T-CHO, total cholesterol; LDL-C, low-density lipoprotein cholesterol; NC, normal control; NP, normal protein; CR, caloric restriction; LP, low-protein.

chronic inflammatory cell infiltration into the renal interstitium. However, the three dietary interventions ameliorated these pathological changes to varying degrees, with the LPCR group demonstrating the most significant effect (Fig. 4A).

Periodic acid-Schiff staining indicated enlarged areas of glycogen deposition in the kidneys of mice in the NP group, along with widening of the mesangial matrix in the glomeruli and thickening of the tubular basement membrane. However, treatment with CR, LP, and LPCR di-

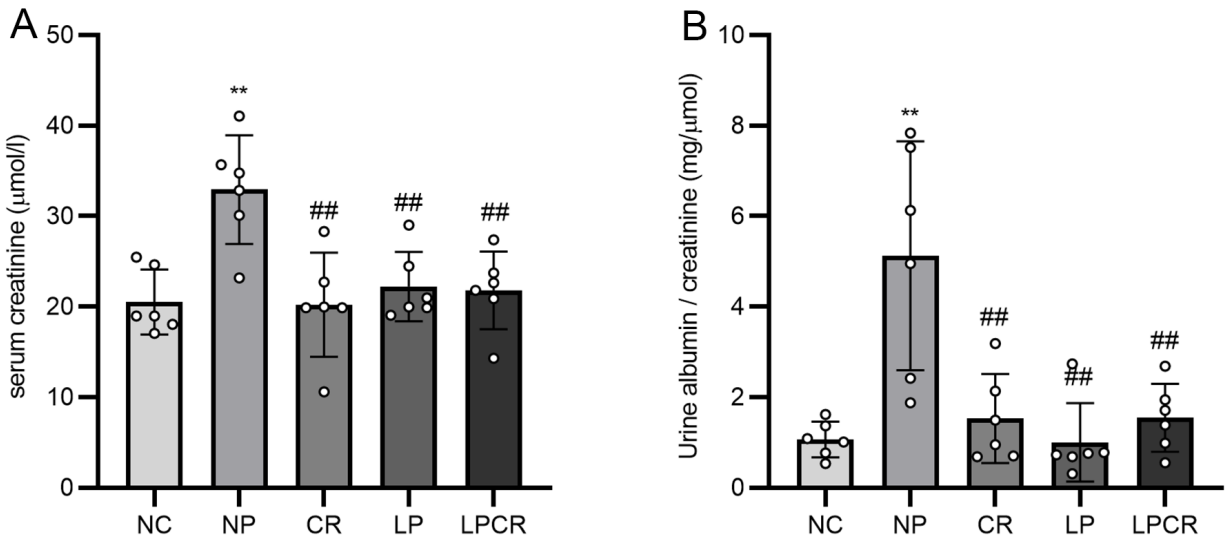

Fig. 3. LPCR diet improves renal function in DKD mice. (A) Mean serum creatinine level and (B) mean urinary albumin-to-creatinine ratio in each group. Values are expressed as mean ± SD, $n = 6$. $^{**}p < 0.01$ vs. NC group; $^{\#\#}p < 0.01$ vs. NP group. LPCR, low-protein calorie-restricted; DKD, diabetic kidney disease; NC, normal control; NP, normal protein; CR, caloric restriction; LP, low-protein.

ets alleviated these pathological alterations to varying degrees, with the LPCR group showing the most significant improvement (Fig. 4B).

Masson's trichrome staining revealed marked collagen accumulation in renal tissues of NP group mice ($p < 0.01$), indicating pronounced renal fibrosis. However, CR, LP, and LPCR dietary interventions significantly attenuated collagen deposition (all $p < 0.01$; Fig. 4C,D). Additionally, immunohistochemical analysis revealed significantly elevated glomerular fibronectin ($p < 0.01$) and renal interstitial collagen I ($p < 0.01$) in the NP group versus NC group. In contrast, the LPCR intervention significantly suppressed the expression of these fibrosis-associated proteins (both $p < 0.01$; Fig. 5).

3.3 LPCR Diet Modulates Gut Microbiota

β-diversity analysis was performed to evaluate gut microbiota compositional similarities across different groups. Notably, the NP group displayed a clear separation from the NC group, indicating significant alterations in microbial diversity. PCoA further revealed that the LPCR group clustered most closely to the NC group. PERMANOVA confirmed the statistically significant differences between dietary interventions ($p < 0.01$; Fig. 6A).

The GMHI, a metric quantifying health-associated microbial signatures via stool metagenomic profiling, showed significant impairment in the NP group compared to the NC group ($p < 0.01$). Notably, the LPCR diet led to a significant improvement in GMHI compared with that in the NP group ($p < 0.01$; Fig. 6B).

To delineate how dietary interventions counteract gut microbiota dysbiosis in DKD mice, we analysed the taxonomic shifts across the phylum, genus, and species levels. At the phylum level, Firmicutes abundance ($p < 0.01$) and Firmicutes/Bacteroidetes (F/B) ratio ($p = 0.017$) were higher in the NP group than those in the NC group. Notably, treatment with the LPCR diet markedly decreased Firmicutes abundance ($p < 0.01$) and F/B ratio ($p = 0.02$) in mice with DKD (Fig. 6C,D). Genus- and species-level analyses further demonstrated significantly increased abundance of *Bacteroides* ($p < 0.01$) and *Bacteroides acidifaciens* ($p < 0.01$), respectively, in the LPCR group versus NP group (Fig. 6E,F).

Given the critical role of TMAO, a gut microbiota-derived metabolite, in renal pathophysiology, we assessed dietary modulation of this uremic toxin. Serum TMAO levels were significantly elevated in the NP group relative to NC group ($p < 0.01$). Conversely, CR, LP, and LPCR dietary interventions demonstrated significant reductions in serum TMAO levels relative to NP group measurements ($p = 0.019$, $p < 0.01$, and $p < 0.01$, respectively), with the LPCR diet exerting the most pronounced inhibitory effect (Fig. 6G).

3.4 LPCR Diet Provides Antioxidant and Anti-inflammatory Benefits

Oxidative stress and systemic inflammation were identified as key mechanisms underlying DKD progression. Compared to the NC group, the NP group exhibited notably reduced serum GSH and SOD levels, along with a marked increase in TNF-α levels (all $p < 0.01$). However, treatment with LPCR diet for five weeks reversed these trends, demonstrating a significant upregulation of GSH and SOD alongside suppression of TNF-α relative to the NP group (all $p < 0.01$; Fig. 7A–C).

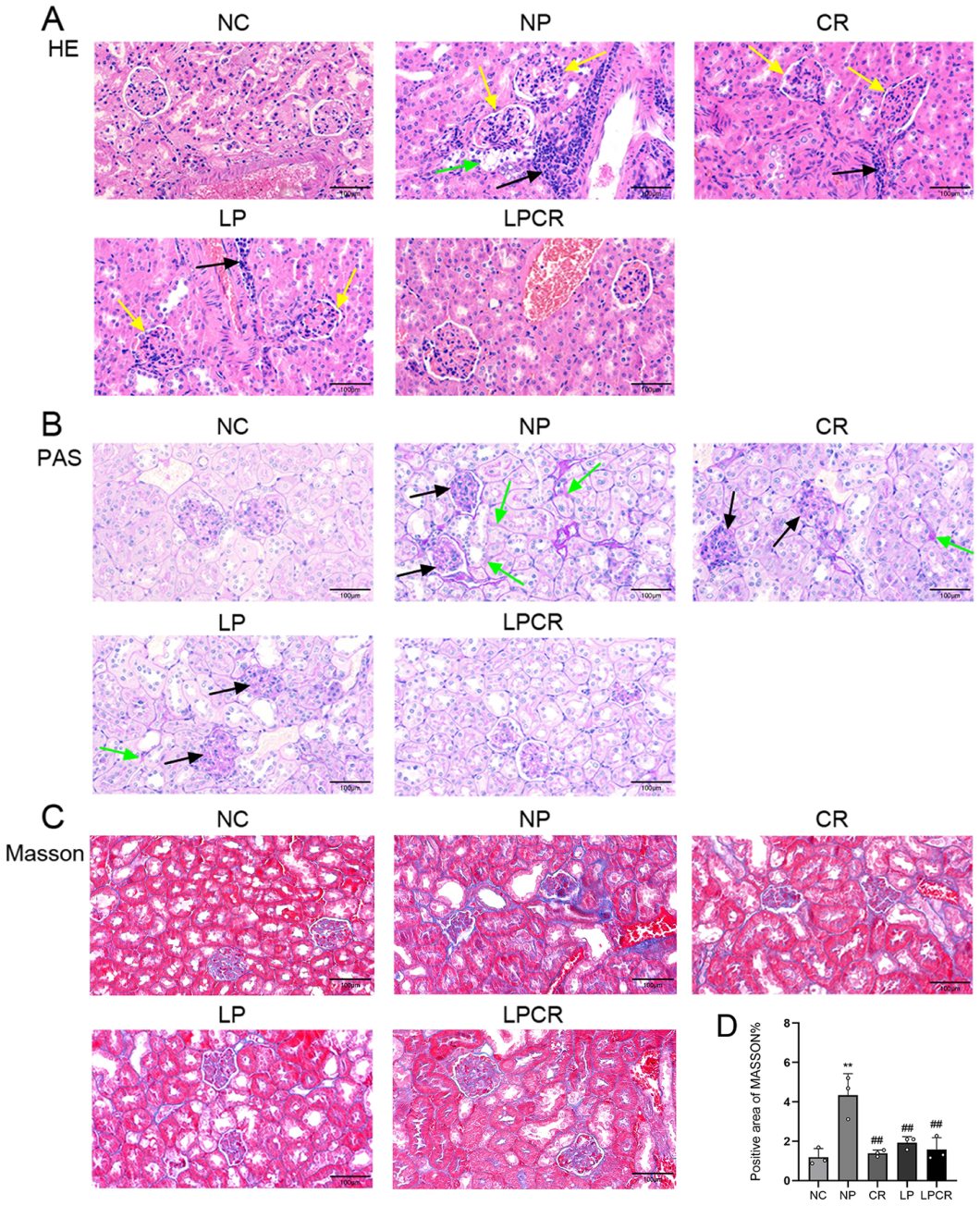

Fig. 4. LPCR diet alleviates partial pathological abnormalities of the kidneys in DKD mice. (A) Representative photomicrographs of Haematoxylin and eosin (HE)-stained kidney sections in each group after dietary intervention. Yellow arrows: irregular glomerular morphology; green arrow: cytoplasmic vacuolation in renal tubular epithelial cell, black arrows: chronic inflammatory cell infiltration in the renal interstitium. Scale bar: 100 µm; original magnification: 200×. (B) Representative photomicrographs of Periodic acid-Schiff (PAS)-stained kidney sections in each group after dietary intervention. Black arrows: mesangial matrix widening in glomeruli; green arrows: renal tubular basement membrane thickening. Magnification = 200×. Scale bar: 100 µm. (C) Representative photomicrographs of Masson's trichrome-stained kidney sections in each group after dietary intervention. Blue-stained areas indicate collagen fiber deposition. Magnification = 200×. Scale bar: 100 µm. (D) Quantitative analysis of the mean collagen fiber area in each group after dietary intervention. Values are expressed as mean ± SD, $n = 3$. $^{**}p < 0.01$ vs. NC group; $^{\#\#}p < 0.01$ vs. NP group. LPCR, low-protein calorie-restricted; DKD, diabetic kidney disease; NC, normal control; NP, normal protein; CR, caloric restriction; LP, low-protein.

Activation of NLRP3 inflammasomes served as a driving factor in immune-inflammatory dysregulation. ASC, NLRP3, and IL-1β expression levels in kidney tissue were markedly higher in the NP group than in the NC group (all $p < 0.01$). Conversely, dietary interventions with CR, LP, and LPCR markedly attenuated the expression of these

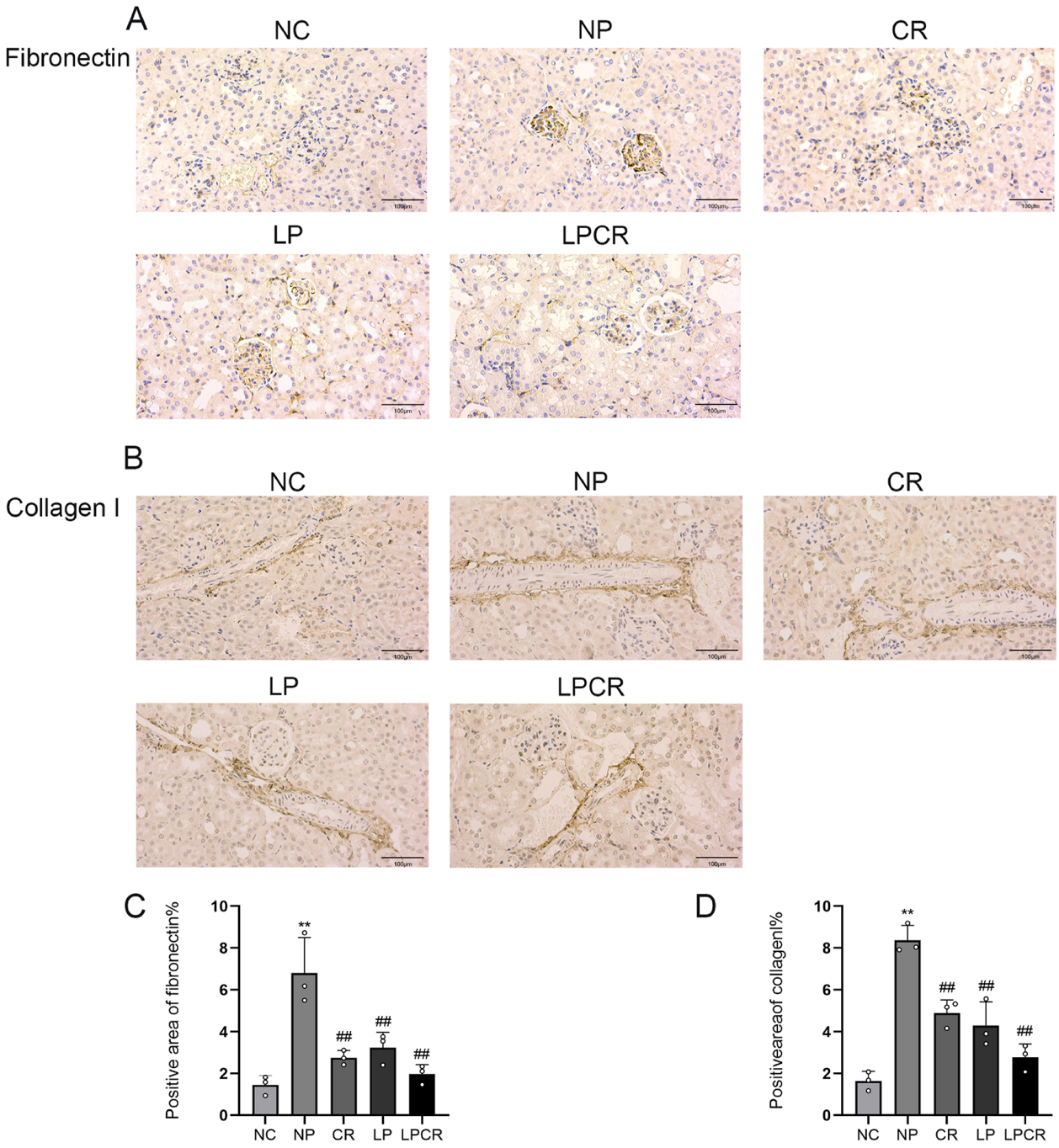

Fig. 5. LPCR diet alleviates renal fibrosis in DKD mice. (A,B) Representative immunohistochemical images of fibronectin (A) and collagen I (B) in each group after dietary intervention. Scale bar: 100 μm; original magnification: 200×. (C,D) Quantitative analysis of the mean positive area of fibronectin (C) and collagen I (D) in each group after dietary intervention. Values are expressed as mean ± SD, $n = 3$. $^{**}p < 0.01$ vs. NC group; $^{\#\#}p < 0.01$ vs. NP group. LPCR, low-protein calorie-restricted; DKD, diabetic kidney disease; NC, normal control; NP, normal protein; CR, caloric restriction; LP, low-protein.

inflammatory markers (all $p < 0.01$), with the LPCR group showing the most pronounced decrease in NLRP3 expression (Fig. 7D–G).

4. Discussion

Our findings indicated that the LPCR diet might exert renoprotective effects, potentially by regulating the gut–kidney axis, characterized by reduced circulating TMAO levels and suppression of NLRP3 inflammasome activa-

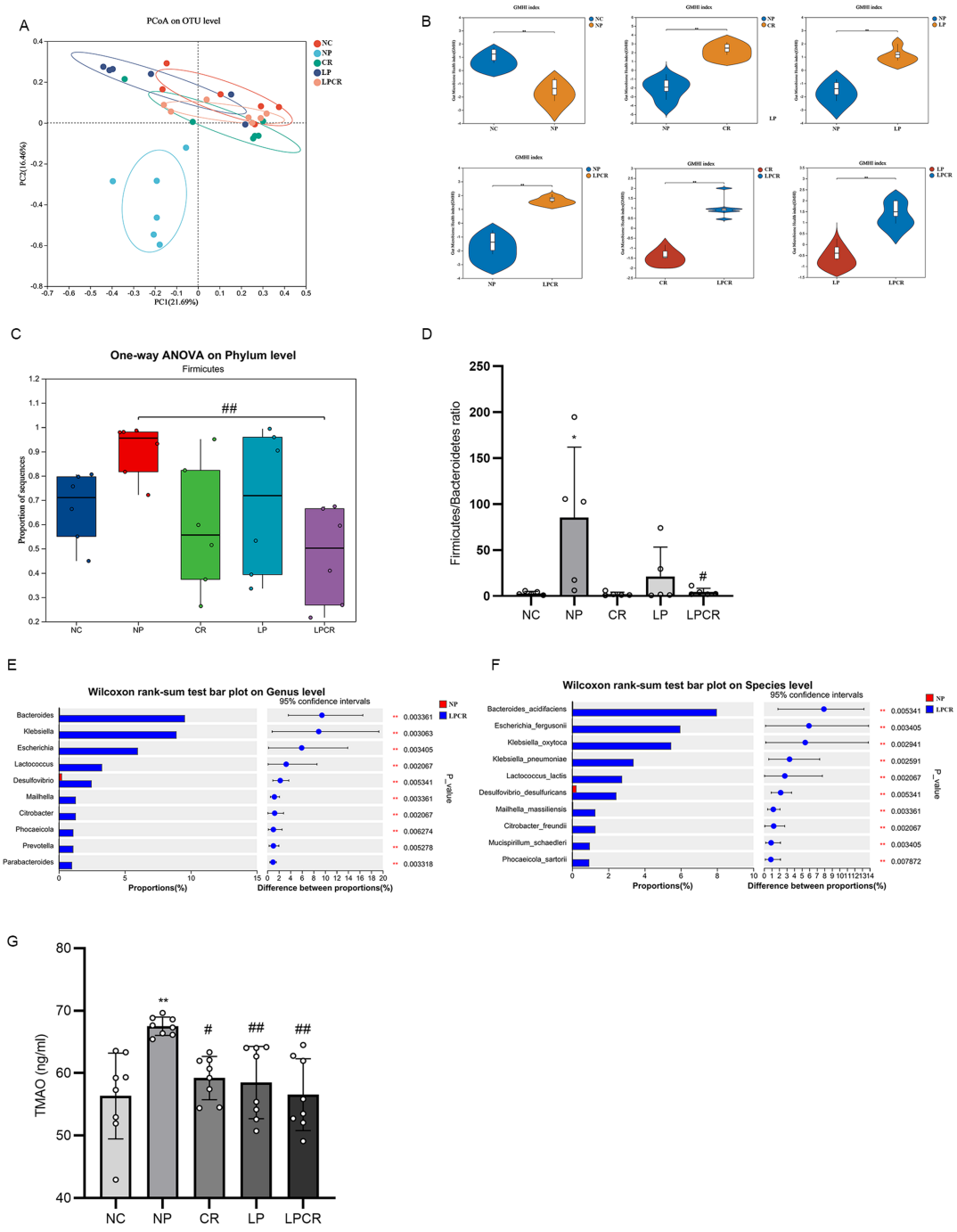

Fig. 6. LPCR diet modulates gut microbiota in DKD mice. (A) Principal coordinate analysis (PCoA) of each group. (B) Comparison of Gut Microbiome Health Index (GMHI) among different groups. (C,D) Mean Firmicutes abundance (C) and mean Firmicutes/Bacteroidetes ratio (D) in each group after dietary intervention. (E,F) Comparison of gut microbiota at the genus level (E) and species level (F) between NP and LPCR groups. (G) Mean serum trimethylamine oxide (TMAO) level in each group after dietary intervention. Values are expressed as mean ± SD, n = 6–8. $^{*}p < 0.05$, $^{**}p < 0.01$ vs. NC group; $^{\#}p < 0.05$, $^{\#\#}p < 0.01$ vs. NP group. LPCR, low-protein calorie-restricted; DKD, diabetic kidney disease; NC, normal control; NP, normal protein; CR, caloric restriction; LP, low-protein.

tion. These results align with Cai *et al.* [16], who reported that dietary resveratrol, a CR mimetic, mitigates renal fibrosis and inflammation in diabetic models via gut microbiota normalization and anti-inflammatory pathway inhibition.

Dysbiosis of the gut microbiota has been implicated in the pathogenesis and progression of multiple conditions, such as type 2 diabetes and CKD [17,18]. CKD can disrupt the gut microbiome's equilibrium, leading to dysbiosis,

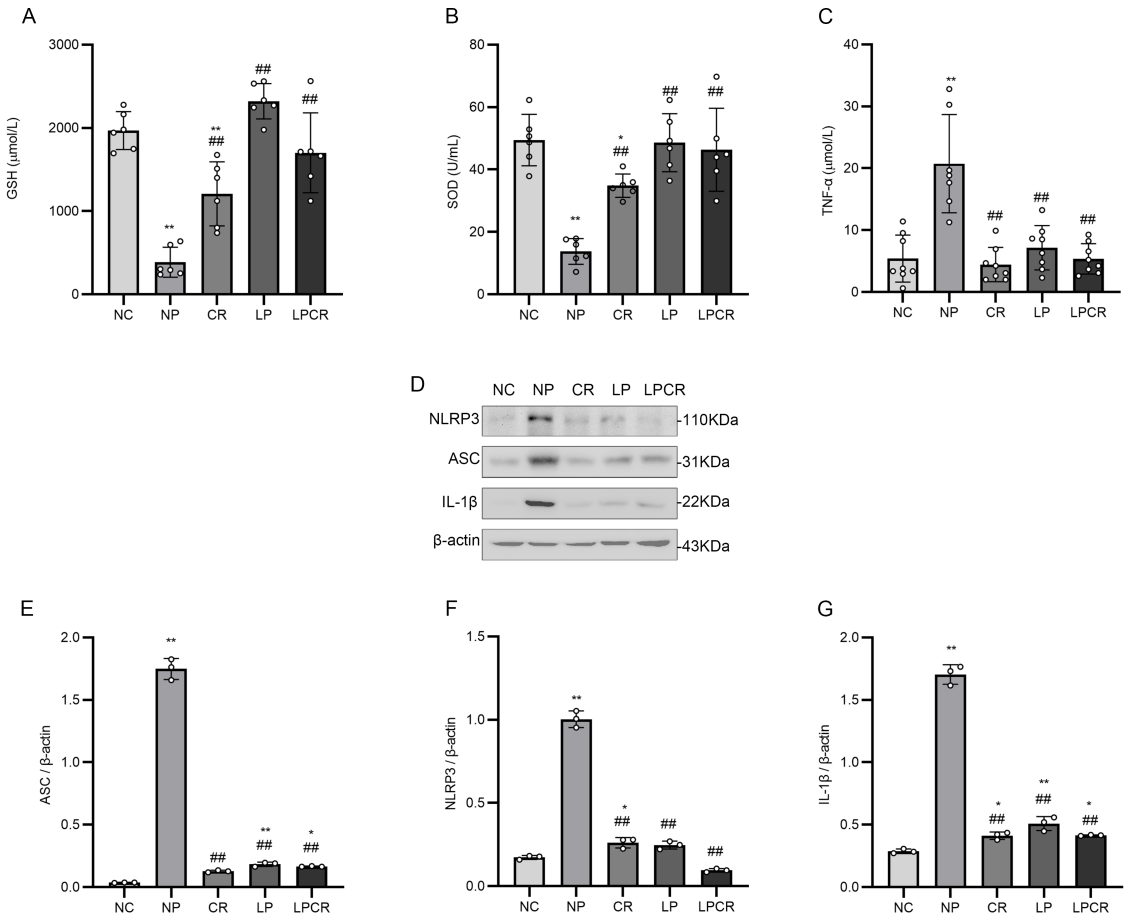

Fig. 7. LPCR diet provides antioxidant and anti-inflammatory benefits in DKD mice. (A–C) Mean GSH level (A), mean SOD level (B), and mean TNF-α level (C) in each group after dietary intervention. (D) Representative Western blot images of NLRP3 inflammasome-related protein in the kidney tissue of DKD mice after dietary intervention. (E–G) Western blot densitometric analysis of ACS (E), NLRP3 (F), and IL-1β (G) in each group after dietary intervention. Values are expressed as mean $\pm$ SD, n = 3–6. $^{*}p < 0.05$, $^{**}p < 0.01$ vs. NC group; $^{\#\#}p < 0.01$ vs. NP group. LPCR, low-protein calorie-restricted; DKD, diabetic kidney disease; GSH, glutathione; SOD, superoxide dismutase; TNF-α, tumor necrosis factor-α; NLRP3, NOD-like receptor family pyrin domain containing 3; ASC, apoptosis-associated speck-like protein containing a CARD; IL-1β, interleukin-1β; NC, normal control; NP, normal protein; CR, caloric restriction; LP, low-protein.

which may further elevate the levels of uraemic toxins and exacerbate CKD progression [19]. Diet significantly influences microbial composition and function [20,21], making dietary interventions a promising strategy for restoring microbial balance in CKD [21]. To evaluate the microbiota's role in the renal benefits of the LPCR diet, we analysed the microbial profiles in diabetic mice across different dietary groups. Distinct shifts in microbial diversity were observed across dietary groups. Notably, the four dominant bacterial groups, Firmicutes, Bacteroidetes, Actinobacteria, and Proteobacteria, collectively comprised over 90% of the gut microbiota, with Firmicutes and Bacteroidetes particularly involved in regulating the host metabolism and immunity [22]. A high abundance of Firmicutes and low abundance of Bacteroidetes is strongly linked with obesity, which is often associated with diabetes [23]. TMAO is a gut-derived toxic metabolite that is associated with increased systemic inflammation. Research findings indicate that high TMAO production is associated with elevated F/B ratios in healthy individuals [24]. Additionally, plasma TMAO levels were negatively correlated with Bacteroides abundance in mice fed high-choline diet [25]. Elevated TMAO levels in patients with CKD are closely associated with decreased renal function [26–28]. Changes in gut microbiota contribute to the development of DKD, with TMAO and chronic inflammation playing pivotal roles in this process [29]. Furthermore, serum TMAO level has been recognised as an independent risk factor for DKD [30]. Notably, the observed suppression of F/B ratios and TMAO levels in LPCR-treated mice directly parallels Cai *et al.*'s [16] findings, reinforcing the pivotal role of gut microbiota remodeling in mitigating diabetic kidney injury. Importantly, our study

advances this paradigm by establishing a novel mechanistic link between LPCR-induced TMAO reduction and downstream NLRP3 inflammasome inhibition—a connection previously unexplored in combined dietary interventions. Unlike prior studies emphasizing isolated protein restriction [4,31] or CR alone [32,33], our study uniquely integrates both interventions, demonstrating superior efficacy in modulating metabolic and inflammatory markers. This synergy suggests that energy imbalance—a critical factor highlighted in recent CR studies [34]—may amplify the benefits of protein restriction by concurrently addressing dysregulated energy metabolism inherent to diabetes. While a randomized controlled trial demonstrated that CR alone induces significant weight loss and anti-inflammatory effects in individuals with metabolic syndrome [35], our mechanistic data extend these observations and suggest that LPCR-driven TMAO reduction may contribute to NLRP3 inflammasome inhibition. This resolves a key gap in understanding how combined CR and LP interventions synergistically ameliorate DKD beyond isolated metabolic improvements, providing a multitargeted therapeutic framework.

Mechanistically, TMAO influences kidney injury primarily through the exacerbation of tubulointerstitial fibrosis and renal inflammation [36–38]. Consistent with this mechanism, a recent study has further elucidated that TMAO enhances TNF-α mediated renal inflammation by stimulating renal fibroblasts to secrete pro-inflammatory mediators, chemokines, and cytokines [39]. Oxidative stress and inflammatory pathways, which mutually reinforce one another, are pivotal in CKD pathogenesis [26]. The NLRP3 inflammasome contributes to CKD advancement, particularly in DKD [40,41]. Research indicates that TMAO can induce oxidative stress and activate the NLRP3-mediated inflammatory pathway, culminating in cytokine release [38,42]. Conversely, the inhibition of TMAO can reduce NLRP3 inflammasome activation and oxidative stress [43]. Our study indicated that LPCR induced the decrease in serum TMAO levels alongside downregulation of ASC, NLRP3, and IL-1β expression, expanding upon Chen *et al.*'s findings [11] on podocyte autophagy by introducing gut-derived metabolites may act as the upstream regulators of renal inflammasomes. Furthermore, our LPCR model addresses a methodological gap in DKD studies, which often focus on macronutrient restriction without considering energy balance. By integrating both calorie and protein restriction, our approach not only improves glycemic control and lipid profiles but also reduces oxidative stress markers, highlighting LPCR's multifactorial benefits compared to transient or single-component dietary interventions [7,9]. Importantly, our results challenge the prevailing view that protein restriction is the primary driver of renal protection [4]. Instead, our data are consistent with the conceptual paradigm proposed by Smith *et al.* [34], which identifies energy imbalance as the central mediator of dietary benefits. This suggests that the efficacy of LPCR may partially originate from sustained negative energy balance rather than from protein restriction itself—a hypothesis that our study further supports through microbiota-mediated mechanistic evidence.

Despite the promising findings, the study had some limitations. For example, we set the protein ratio for the LPCR group to 13% protein with 30% CR to prevent protein-energy wastage. Previous animal studies have shown that intermittent very low-protein diet [44], 50% CR [7], and intermittent CR [7] can improve DKD. Therefore, further research is needed to determine the optimal protein ratio for LPCR and explore whether intermittent approaches are more effective. Additionally, owing to the prolonged modelling period for DKD and other constraints, we did not conduct counterevidence experiments, limiting our ability to clearly define the direct effects of differential bacterial species on TMAO levels. In future studies, we plan to address this limitation by employing fecal microbiota transplantation or other counterevidence techniques to verify the regulatory effects of Firmicutes and Bacteroidetes on TMAO and DKD.

5. Conclusions

The LPCR diet mitigates kidney injury in diabetic mice, potentially by regulating the gut–kidney axis. This protective effect may stem from reduced circulating TMAO levels, which subsequently inhibit NLRP3 inflammasome activation in kidney tissue. Overall, this study provides the foundation for further research on the specific mechanisms by which LPCR diet regulates the gut–kidney axis, offering new insights and strategies for the clinical treatment of DKD.

Disclosure

The paper is listed as "Low-protein Calorie-restriction Mitigates Diabetic Mice Kidney Injury via the Gut–Kidney Axis" as a preprint on (ResearchGate) at https://www.researchgate.net/publication/386399913_A_low-protein_calorie-restricted_diet_mitigates_kidney_injury_in_diabetic_mice_by_modulating_the_gut-kidney_axis.

Abbreviations

CKD, Chronic kidney disease; CR, Caloric restriction; DKD, Diabetic kidney disease; GSH, Glutathione; HDL-C, High-density lipoprotein cholesterol; LDL-C, Low-density lipoprotein cholesterol; LP, Low-protein; LPCR, Low-protein calorie-restricted; NP, Normal protein; SOD, Superoxide dismutase; TMAO, Trimethylamine oxide; TG, Triglycerides; T-CHO, Total cholesterol.

Availability of Data and Materials

The data that support the findings of this study are available from the corresponding authors on reasonable request.

Author Contributions

RXZ and XW contributed to formal analysis, investigation, draft preparation, and visualization. YJX contributed to data curation. CRH and XZC contributed to image acquisition and analysis. YLW contributed to statistical analyses. YG contributed to funding acquisition, project administration, writing and review, and editing. YG and CL contributed to conceptualization, validation, and supervision. All authors read and approved the final manuscript. All authors contributed to editorial changes in the manuscript. All authors have participated sufficiently in the work and agreed to be accountable for all aspects of the work.

Ethics Approval and Consent to Participate

All animal experiments were approved by the Animal Experiment Ethics Committee of the Affiliated Hospital of Nanjing University of Chinese Medicine (Ethics No. AEWC-20230531-309) and complied with the Guidelines for the Care and Use of Animals established by the Chinese Animal Management Committee.

Acknowledgment

The skillful technical assistance of Yu Chen, Xingjia Li, Qifeng Wang, Houcai Huang, Rongling Zhong, and Zhi Xia is appreciated.

Funding

This work was supported by Clinical Medicine Science and Technology Development Fund Project of Jiangsu University (JLY2021162), "Double Innovation Doctor" of Jiangsu Province (JSSCBS20211615), and Special Research Startup Funding for Introduced Personnel of Nanjing Lishui People's Hospital (KY07).

Conflict of Interest

The authors declare no conflict of interest.

Supplementary Material

Supplementary material associated with this article can be found, in the online version, at https://doi.org/10.31083/IJVNR37311.

References

[1] Kikuchi K, Saigusa D, Kanemitsu Y, Matsumoto Y, Thanai P, Suzuki N, *et al*. Gut microbiome-derived phenyl sulfate contributes to albuminuria in diabetic kidney disease. Nature Communications. 2019; 10: 1835. https://doi.org/10.1038/s41467-019-09735-4.

[2] Mao ZH, Gao ZX, Liu DW, Liu ZS, Wu P. Gut microbiota and its metabolites - molecular mechanisms and management strategies in diabetic kidney disease. Frontiers in Immunology. 2023; 14: 1124704. https://doi.org/10.3389/fimmu.2023.1124704.

[3] Chen YY, Chen DQ, Chen L, Liu JR, Vaziri ND, Guo Y, *et al*. Microbiome-metabolome reveals the contribution of gut-kidney axis on kidney disease. Journal of Translational Medicine. 2019; 17: 5. https://doi.org/10.1186/s12967-018-1756-4.

[4] Kitada M, Ogura Y, Monno I, Koya D. A Low-Protein Diet for Diabetic Kidney Disease: Its Effect and Molecular Mechanism, an Approach from Animal Studies. Nutrients. 2018; 10: 544. https://doi.org/10.3390/nu10050544.

[5] Fontana L, Partridge L, Longo VD. Extending healthy life span–from yeast to humans. Science (New York, N.Y.). 2010; 328: 321–326. https://doi.org/10.1126/science.1172539.

[6] Wang SY, Cai GY, Chen XM. Energy restriction in renal protection. The British Journal of Nutrition. 2018; 120: 1149–1158. https://doi.org/10.1017/S0007114518002684.

[7] Eid SA, O'Brien PD, Kretzler KH, Jang DG, Mendelson FE, Hayes JM, *et al*. Dietary interventions improve diabetic kidney disease, but not peripheral neuropathy, in a db/db mouse model of type 2 diabetes. FASEB Journal: Official Publication of the Federation of American Societies for Experimental Biology. 2023; 37: e23115. https://doi.org/10.1096/fj.202300354R.

[8] Kitada M, Takeda A, Nagai T, Ito H, Kanasaki K, Koya D. Dietary restriction ameliorates diabetic nephropathy through anti-inflammatory effects and regulation of the autophagy via restoration of Sirt1 in diabetic Wistar fatty (fa/fa) rats: a model of type 2 diabetes. Experimental Diabetes Research. 2011; 2011: 908185. https://doi.org/10.1155/2011/908185.

[9] Giordani I, Malandrucco I, Donno S, Picconi F, Di Giacinto P, Di Flaviani A, *et al*. Acute caloric restriction improves glomerular filtration rate in patients with morbid obesity and type 2 diabetes. Diabetes & Metabolism. 2014; 40: 158–160. https://doi.org/10.1016/j.diabet.2013.12.006.

[10] Ruggenenti P, Cortinovis M, Trillini M, Parvanova A, Abbate M, Satriano C, *et al*. Long-term kidney and systemic effects of calorie restriction in overweight or obese type 2 diabetic patients (C.Re.S.O. 2 randomized controlled trial). Diabetes Research and Clinical Practice. 2022; 185: 109804. https://doi.org/10.1016/j.diabres.2022.109804.

[11] Chen GF, Geng Y, Liu C. A low-protein calorie-restricted diet attenuates renal injury and facilitates podocyte autophagy in type 2 diabetic rats. Diabetes. 2018; 67: 514-P. https://doi.org/10.2337/db18-514-P.

[12] Clemente JC, Ursell LK, Parfrey LW, Knight R. The impact of the gut microbiota on human health: an integrative view. Cell. 2012; 148: 1258–1270. https://doi.org/10.1016/j.cell.2012.01.035.

[13] Zheng X, Wang S, Jia W. Calorie restriction and its impact on gut microbial composition and global metabolism. Frontiers of Medicine. 2018; 12: 634–644. https://doi.org/10.1007/s11684-018-0670-8.

[14] Black AP, Anjos JS, Cardozo L, Carmo FL, Dolenga CJ, Nakao LS, *et al*. Does Low-Protein Diet Influence the Uremic Toxin Serum Levels From the Gut Microbiota in Nondialysis Chronic Kidney Disease Patients? Journal of Renal Nutrition: the Official Journal of the Council on Renal Nutrition of the National Kidney Foundation. 2018; 28: 208–214. https://doi.org/10.1053/j.jrn.2017.11.007.

[15] Gupta VK, Kim M, Bakshi U, Cunningham KY, Davis JM, 3rd, Lazaridis KN, *et al*. A predictive index for health status using species-level gut microbiome profiling. Nature Communications. 2020; 11: 4635. https://doi.org/10.1038/s41467-020-18476-8.

[16] Cai TT, Ye XL, Li RR, Chen H, Wang YY, Yong HJ, *et al*. Resveratrol Modulates the Gut Microbiota and Inflammation to Protect Against Diabetic Nephropathy in Mice. Frontiers in Pharmacology. 2020; 11: 1249. https://doi.org/10.3389/fphar.2020.01249.

[17] Qin J, Li Y, Cai Z, Li S, Zhu J, Zhang F, *et al*. A metagenome-wide association study of gut microbiota in type 2 diabetes. Nature. 2012; 490: 55–60. https://doi.org/10.1038/nature11450.

[18] Vaziri ND, Zhao YY, Pahl MV. Altered intestinal microbial flora and impaired epithelial barrier structure and function in CKD: the nature, mechanisms, consequences and potential treatment. Nephrology, Dialysis, Transplantation: Official Publication of the European Dialysis and Transplant Association - European

Renal Association. 2016; 31: 737–746. https://doi.org/10.1093/ndt/gfv095.

[19] Cabała S, Ożgo M, Herosimczyk A. The Kidney-Gut Axis as a Novel Target for Nutritional Intervention to Counteract Chronic Kidney Disease Progression. Metabolites. 2024; 14: 78. https://doi.org/10.3390/metabo14010078.

[20] Zoetendal EG, de Vos WM. Effect of diet on the intestinal microbiota and its activity. Current Opinion in Gastroenterology. 2014; 30: 189–195. https://doi.org/10.1097/MOG.0000000000000048.

[21] Evenepoel P, Poesen R, Meijers B. The gut-kidney axis. Pediatric Nephrology (Berlin, Germany). 2017; 32: 2005–2014. https://doi.org/10.1007/s00467-016-3527-x.

[22] Fujisaka S, Watanabe Y, Tobe K. The gut microbiome: a core regulator of metabolism. The Journal of Endocrinology. 2023; 256: e220111. https://doi.org/10.1530/JOE-22-0111.

[23] Ma Q, Li Y, Li P, Wang M, Wang J, Tang Z, *et al*. Research progress in the relationship between type 2 diabetes mellitus and intestinal flora. Biomedicine & Pharmacotherapy = Biomedecine & Pharmacotherapie. 2019; 117: 109138. https://doi.org/10.1016/j.biopha.2019.109138.

[24] Cho CE, Taesuwan S, Malysheva OV, Bender E, Tulchinsky NF, Yan J, *et al*. Trimethylamine-N-oxide (TMAO) response to animal source foods varies among healthy young men and is influenced by their gut microbiota composition: A randomized controlled trial. Molecular Nutrition & Food Research. 2017; 61: 10.1002/mnfr.201600324. https://doi.org/10.1002/mnfr.201600324.

[25] Wang X, Li X, Dong Y. Vitamin D Decreases Plasma Trimethylamine-N-oxide Level in Mice by Regulating Gut Microbiota. BioMed Research International. 2020; 2020: 9896743. https://doi.org/10.1155/2020/9896743.

[26] El-Deeb OS, Atef MM, Hafez YM. The interplay between microbiota-dependent metabolite trimethylamine N-oxide, Transforming growth factor β/SMAD signaling and inflammasome activation in chronic kidney disease patients: A new mechanistic perspective. Journal of Cellular Biochemistry. 2019; 120: 14476–14485. https://doi.org/10.1002/jcb.28707.

[27] Tang WHW, Wang Z, Kennedy DJ, Wu Y, Buffa JA, Agatisa-Boyle B, *et al*. Gut microbiota-dependent trimethylamine N-oxide (TMAO) pathway contributes to both development of renal insufficiency and mortality risk in chronic kidney disease. Circulation Research. 2015; 116: 448–455. https://doi.org/10.1161/CIRCRESAHA.116.305360.

[28] Missailidis C, Hällqvist J, Qureshi AR, Barany P, Heimbürger O, Lindholm B, *et al*. Serum Trimethylamine-N-Oxide Is Strongly Related to Renal Function and Predicts Outcome in Chronic Kidney Disease. PloS One. 2016; 11: e0141738. https://doi.org/10.1371/journal.pone.0141738.

[29] Yang M, Zhang R, Zhuang C, Wu Y, Yang Q, Yu Z, *et al*. Serum Trimethylamine N-oxide and the Diversity of the Intestinal Microbial Flora in Type 2 Diabetes Complicated by Diabetic Kidney Disease. Clinical Laboratory. 2022; 68: 10.7754/Clin.Lab.2021.210836. https://doi.org/10.7754/Clin.Lab.2021.210836.

[30] Huang Y, Zhu Z, Huang Z, Zhou J. Elevated serum trimethylamine oxide levels as potential biomarker for diabetic kidney disease. Endocrine Connections. 2023; 12: e220542. https://doi.org/10.1530/EC-22-0542.

[31] Ferraz-Bannitz R, Beraldo RA, Peluso AA, Dall M, Babaei P, Foglietti RC, *et al*. Dietary Protein Restriction Improves Metabolic Dysfunction in Patients with Metabolic Syndrome in a Randomized, Controlled Trial. Nutrients. 2022; 14: 2670. https://doi.org/10.3390/nu14132670.

[32] Mihaylova MM, Chaix A, Delibegovic M, Ramsey JJ, Bass J, Melkani G, *et al*. When a calorie is not just a calorie: Diet quality and timing as mediators of metabolism and healthy aging. Cell Metabolism. 2023; 35: 1114–1131. https://doi.org/10.1016/j.cmet.2023.06.008.

[33] Zainordin NA, Eddy Warman NA, Mohamad AF, Abu Yazid FA, Ismail NH, Chen XW, *et al*. Safety and efficacy of very low carbohydrate diet in patients with diabetic kidney disease-A randomized controlled trial. PloS One. 2021; 16: e0258507. https://doi.org/10.1371/journal.pone.0258507.

[34] Smith DL, Jr, Mitchell SE, Johnson MS, Gibbs VK, Dickinson S, Henschel B, *et al*. Benefits of calorie restriction in mice are mediated via energy imbalance, not absolute energy or protein intake. GeroScience. 2024; 46: 4809–4826. https://doi.org/10.1007/s11357-024-01166-4.

[35] Montefusco L, D'Addio F, Loretelli C, Ben Nasr M, Garziano M, Rossi A, *et al*. Anti-inflammatory effects of diet and caloric restriction in metabolic syndrome. Journal of Endocrinological Investigation. 2021; 44: 2407–2415. https://doi.org/10.1007/s40618-021-01547-y.

[36] Zhang W, Miikeda A, Zuckerman J, Jia X, Charugundla S, Zhou Z, *et al*. Inhibition of microbiota-dependent TMAO production attenuates chronic kidney disease in mice. Scientific Reports. 2021; 11: 518. https://doi.org/10.1038/s41598-020-80063-0.

[37] Kapetanaki S, Kumawat AK, Persson K, Demirel I. The Fibrotic Effects of TMAO on Human Renal Fibroblasts Is Mediated by NLRP3, Caspase-1 and the PERK/Akt/mTOR Pathway. International Journal of Molecular Sciences. 2021; 22: 11864. https://doi.org/10.3390/ijms222111864.

[38] Fang Q, Zheng B, Liu N, Liu J, Liu W, Huang X, *et al*. Trimethylamine N-Oxide Exacerbates Renal Inflammation and Fibrosis in Rats With Diabetic Kidney Disease. Frontiers in Physiology. 2021; 12: 682482. https://doi.org/10.3389/fphys.2021.682482.

[39] Stefania K, Ashok KK, Geena PV, Katarina P, Isak D. TMAO enhances TNF-α mediated fibrosis and release of inflammatory mediators from renal fibroblasts. Scientific Reports. 2024; 14: 9070. https://doi.org/10.1038/s41598-024-58084-w.

[40] Ram C, Jha AK, Ghosh A, Gairola S, Syed AM, Murty US, *et al*. Targeting NLRP3 inflammasome as a promising approach for treatment of diabetic nephropathy: Preclinical evidences with therapeutic approaches. European Journal of Pharmacology. 2020; 885: 173503. https://doi.org/10.1016/j.ejphar.2020.173503.

[41] Qiu YY, Tang LQ. Roles of the NLRP3 inflammasome in the pathogenesis of diabetic nephropathy. Pharmacological Research. 2016; 114: 251–264. https://doi.org/10.1016/j.phrs.2016.11.004.

[42] Ke Y, Li D, Zhao M, Liu C, Liu J, Zeng A, *et al*. Gut flora-dependent metabolite Trimethylamine-N-oxide accelerates endothelial cell senescence and vascular aging through oxidative stress. Free Radical Biology & Medicine. 2018; 116: 88–100. https://doi.org/10.1016/j.freeradbiomed.2018.01.007.

[43] Boini KM, Hussain T, Li PL, Koka S. Trimethylamine-N-Oxide Instigates NLRP3 Inflammasome Activation and Endothelial Dysfunction. Cellular Physiology and Biochemistry: International Journal of Experimental Cellular Physiology, Biochemistry, and Pharmacology. 2017; 44: 152–162. https://doi.org/10.1159/000484623.

[44] Kitada M, Ogura Y, Suzuki T, Monnno I, Kanasaki K, Watanabe A, *et al*. Cyclic and intermittent very low-protein diet can have beneficial effects against advanced diabetic nephropathy in Wistar fatty (fa/fa) rats, an animal model of type 2 diabetes and obesity. Nephrology (Carlton, Vic.). 2017; 22: 1030–1034. https://doi.org/10.1111/nep.13152.